



HAL
open science

Methanol oxidation in dry and humid air by dielectric barrier discharge plasma combined with MnO₂–CuO based catalysts

Caroline Norsic, Jean-Michel Tatibouet, Catherine Batiot-Dupeyrat, Elodie Fourré

► **To cite this version:**

Caroline Norsic, Jean-Michel Tatibouet, Catherine Batiot-Dupeyrat, Elodie Fourré. Methanol oxidation in dry and humid air by dielectric barrier discharge plasma combined with MnO₂–CuO based catalysts. *Chemical Engineering Journal*, 2018, 347, pp.944-952. 10.1016/j.cej.2018.04.065 . hal-02148328

HAL Id: hal-02148328

<https://hal.science/hal-02148328>

Submitted on 30 Nov 2020

HAL is a multi-disciplinary open access archive for the deposit and dissemination of scientific research documents, whether they are published or not. The documents may come from teaching and research institutions in France or abroad, or from public or private research centers.

L'archive ouverte pluridisciplinaire **HAL**, est destinée au dépôt et à la diffusion de documents scientifiques de niveau recherche, publiés ou non, émanant des établissements d'enseignement et de recherche français ou étrangers, des laboratoires publics ou privés.

1 Methanol oxidation in dry and humid air by dielectric barrier discharge plasma combined with
2 MnO₂-CuO based catalysts

3 Caroline Norsic^a, Jean-Michel Tatibouët^a, Catherine Batiot-Dupeyrat^a, Elodie Fourré^a

4 ^a Institut de Chimie des Milieux et Matériaux de Poitiers (IC2MP), UMR CNRS 7285
5 Université de Poitiers, Ecole Nationale Supérieure d'Ingénieurs de Poitiers (ENSIP)
6 1, rue marcel Doré, TSA 41105, 86073 Poitiers cedex 9 (France)

7 Corresponding author: elodie.fourre@univ-poitiers.fr

8 Other authors: caroline.norsic@univ-orleans.fr

9 jean.michel.tatibouet@univ-poitiers.fr

10 Catherine.batiot.dupeyrat@univ-poitiers.fr

11

12 Keywords

13 Non thermal plasma, humidity, methanol, oxidation, metal oxide, TPR, ozone

14 Highlights

- 15 • Humidity in plasma alone enhanced CO₂ selectivity
- 16 • 5% MnO₂/5% CuO/Al₂O₃ balls catalyst presented the best activities
- 17 • Hydroperoxide species and/or adsorbed H₂O₂ more selective to CO₂ formation
- 18 • High flow rate treatment of low pollutant concentration is achievable with scaling up

19

20

21

22

1 Abstract

2 Presence of humidity in polluted gas streams is a key parameter to give a realistic view of a
3 depollution process efficiency. With this in mind, the elimination of methanol by non thermal
4 plasma in presence of a MnO₂-CuO based catalyst and 35 % relative humidity (20°C,
5 atmospheric pressure) was achieved. The reactor allows the treatment of low concentration
6 pollutants (25-200 ppm) at weak residence time (0.36s) in air at atmospheric pressure. Based
7 on conversion rate and CO₂ selectivity, a 5 % MnO₂/ 5 % CuO/ Al₂O₃ catalyst was selected
8 within an array of catalysts prepared by different impregnation methods with various metal
9 oxide ratios. The presence of humidity affected methanol conversion, ozone concentration and
10 selectivities to by-products. Beneficial effects of humidity were observed on by-products
11 elimination and CO₂ selectivity despite a lower methanol conversion compared to dry air
12 conditions.

13

1. Introduction

Within the possible decontamination ways to clean gas exhaust, non thermal atmospheric plasma (NTAP) is a renowned process, that does no longer need to prove its worth and has been applied to the treatment of numerous polluted gases with a large diversity of reactor configurations [1-3]. In fact, NTAP shows a high efficiency when treating effluents with low concentration pollutants (ppm level). Within the diversity of species generated in an air plasma, atomic oxygen, nitrogen and, in presence of humidity, OH radicals are produced. These highly reactive species react with each other and with other molecules present in the gas phase to generate ozone and trigger radical oxidation reactions if organic molecules such as volatile organic compounds (VOC) are present. These oxidation processes allows the elimination of pollutants present in air. However, NTAP suffers from several drawbacks such as weak energy efficiency, mineralization and generation of ozone and nitrous oxides (NO_x). One way, which has been developed extensively, to overcome these disadvantages is by placing a catalyst inside or post discharge. Depending on the VOC chemical structure, non-thermal plasma reactor layout and catalyst chemical nature, several conclusions were drawn in respect of VOC removal efficiency (RE), ozone concentration, carbon mass balance (CMB), by-products selectivities, specific energy or discharge behavior [4-14]. Treatment by non thermal plasma alone succeeds in removing low concentration pollutants at low energy consumption compared to conventional catalytic processes. However, the process is sensitive to humidity and since it is non selective, unwanted by-products are generated (ozone, NO_x , amongst others depending on the pollutant). When a catalyst is placed in the plasma discharge, and depending of its chemical nature, a synergistic effect is observed leading to high removal efficiencies. In post plasma configuration, it improves the oxidation reactions by ozone activation leading to higher carbon oxides (CO_x) selectivities and low residual ozone concentration.

1 Additionally, it is difficult to dissociate humidity levels from gas emission when controlling
2 the levels of contaminated air flows, under real operating conditions, arising either from
3 industrial or household environments. When treatment of polluted gas is considered, either via
4 classical (thermal, catalytic oxidation, adsorption...) or slightly more unconventional ways
5 (such as non thermal plasma, photocatalysis...), water should be taken into account, as it will
6 affect the reaction selectivities and efficiencies.

7 In a plasma alone configuration, when no catalyst was present in the discharge or post
8 discharge, opposite effects were observed depending on the relative humidity (RH)
9 percentages present in the gas stream [4, 7, 12, 13]. In a low humid environment, the
10 formation of highly oxidative hydroxyl radicals ($\cdot\text{OH}$) increases due to the dissociation of
11 water molecules by impact with electrons or oxygen radicals, $\text{O}(1\text{D})$. Ono and Oda [15]
12 measured the $\cdot\text{OH}$ concentration as a function of humidity and observed a maximum [$\cdot\text{OH}$] at
13 $\text{RH} < 1\%$ in a pulsed corona discharge. In the case of toluene elimination [4], since $\cdot\text{OH}$
14 radicals have the highest reaction rate coefficient ($k = 5.7 \times 10^{-12} \text{ molecule cm}^{-3} \cdot \text{s}^{-1}$) within the
15 group of plasma oxidizing species (for atomic oxygen $k = 7.6 \times 10^{-14} \text{ molecule cm}^{-3} \cdot \text{s}^{-1}$ and
16 ozone $k = 3.9 \times 10^{-22} \text{ molecule cm}^{-3} \cdot \text{s}^{-1}$), an increase of the VOC removal efficiency was
17 observed. Depending on the type of plasma reactor and pollutant treated, a positive effect on
18 the removal efficiency (RE) was detected with fairly different RH contents. Lock et al. [12]
19 observed an increase of the RE with RH up to 2 % in a corona reactor for methanol and
20 dimethyl sulfide elimination. Regarding the treatment of toluene effluent, the limit was drawn
21 at 0.2 % (mol %) in a dielectric barrier discharge (DBD) wire plate reactor [13], 26 % in a
22 direct current (DC) positive corona discharge [4]. Surprisingly, Karatum et al. [7] showed that
23 a RH of 30 % did not alter the RE of ethylbenzene in a volumic cylindrical DBD.

24 However, removal efficiencies and ozone concentrations are decreasing when the relative
25 humidity exceeds the values cited above, independently of the reactor configuration or VOC.

1 Several arguments were given to explain this phenomena. Water content has a strong impact
2 on the plasma discharge electronic density. Excess humidity limits the current at constant
3 applied voltage due to the modification of dielectric's surface resistance and reduces the
4 transferred charges between the electrodes and thus reducing of the volume of plasma [14].
5 Additionally, a reduction of highly energetic electrons concentration was observed due to
6 their inelastic collisions with water molecules [15]. These arguments were confirmed by other
7 authors such as Van Durme et al. [4]. They reported that toluene abatement, in a plasma alone
8 configuration, was enhanced in presence of relatively low RH contents (25 - 27 %). However,
9 at higher humidity levels (50 %), this effect was impeded by the reduction of the plasma
10 electric field and mobility of charge carriers in presence of water, thus altering the discharge
11 chemical composition [4, 16]. If the advantage of increasing $\cdot\text{OH}$ radical content with low
12 humidity levels improved the removal efficiency, this effect was counteracted at higher RH
13 due to the decrease of the number of microdischarges, especially for VOCs that can be
14 directly decomposed by electronic impact. Furthermore, the ozone formation in the plasma
15 discharge was reduced under the influence of humidity. $\text{O} (^1\text{D})$ radicals (from O_2 dissociation)
16 reacts with H_2O to produce $\cdot\text{OH}$ radicals. The $\text{H}\cdot$ radicals issued from water dissociation can
17 also account for the increased HO_2 formation. The resulting $\text{H}\cdot$, $\cdot\text{OH}$ and $\cdot\text{HO}_2$ are responsible
18 for the decrease of ozone concentration. These radicals react with ozone to form O_2 [4, 17,
19 18]. By-products, CO_x selectivities and carbon balance were also modified by the RH. If
20 water showed a negative effect on the RE, it improved by-products oxidation, carbon balance
21 and CO_x selectivities [12, 13, 19].

22 When a catalyst is combined to the plasma under humid conditions, in plasma or post plasma,
23 a decrease of the VOC removal efficiency was observed, independently of reactor type or
24 VOC chemical structure [5, 6, 8–11, 18]. The beneficial effect of the catalyst was hindered by
25 surface coverage with water molecules thus limiting access to active sites [6, 8, 18–20].

1 Sivachandiran et al. [8] reported a very detailed study on the effect of humidity on
2 isopropanol adsorption on TiO₂ surface and its ensuing non thermal plasma treatment. They
3 showed that isopropanol adsorption was affected by humidity in different ways according to
4 the RH level. Below 35 %, a decrease of adsorption was observed with increasing RH due to
5 the competition between water and VOC for adsorption on surface sites. Above 35 %, the
6 decrease of adsorption with RH was also observed with an increase of irreversible isopropanol
7 adsorption. It was suggested that above 35 % humidity level the surface is covered by one
8 monolayer of water [21] and the irreversible adsorption could be partially due to solvated IPA
9 isopropanol. Under plasma treatment, the RH content improved isopropanol desorption due to
10 the rehydroxylation of the catalyst surface by ·OH radical and ensuing swap of isopropanol
11 molecules to OH. If dichloromethane and toluene contaminated effluents encountered a more
12 or less important drop in their conversion in presence of water (2 mol %), it was surprising
13 that methanol (CH₃OH) was almost not affected by water content in a ferroelectric packed
14 bed reactor (FPR) containing BaTiO₃ pellets [9]. Conclusions were drawn on the basis that the
15 plasma treatment activated directly CH₃OH which converted rapidly into formaldehyde then
16 to CO, with little H₂O contribution. Regarding the enhanced selectivity to CO₂ in presence of
17 water, a direct transformation of intermediates to CO₂, and not from CO oxidation was
18 proposed. Selectivities to CO₂ and carbon balance were enhanced in presence of a catalyst in
19 18 % humidity for TCE abatement as shown by Dinh et al. [19], in over 35 % RH for IPA
20 elimination [8], 2% RH for dichloromethane, toluene and methanol [9].

21 It appears from all these studies that humidity presents contradictory effects regarding the
22 VOC conversion, ozone concentration and selectivities of chemical reactions, depending on
23 the VOC nature and plasma reactor configuration with or without a catalyst. A statement
24 found in every publication, although, is the decrease of pollutant removal efficiency at high
25 humidity levels (>30 %) due to 3 major factors: 1- decrease of the electronic density of the

1 plasma discharge thus decreasing the active species energy and concentration; 2- surface
2 coverage of the catalyst by water molecules reducing the adsorption process of pollutant and
3 active sites availability; 3- reduction of the ozone concentration, strong oxidant in catalytic
4 process. Increased $\cdot\text{OH}$ radical concentration, despite its high reactivity, cannot supplant, in
5 many cases, the loss of reactivity.

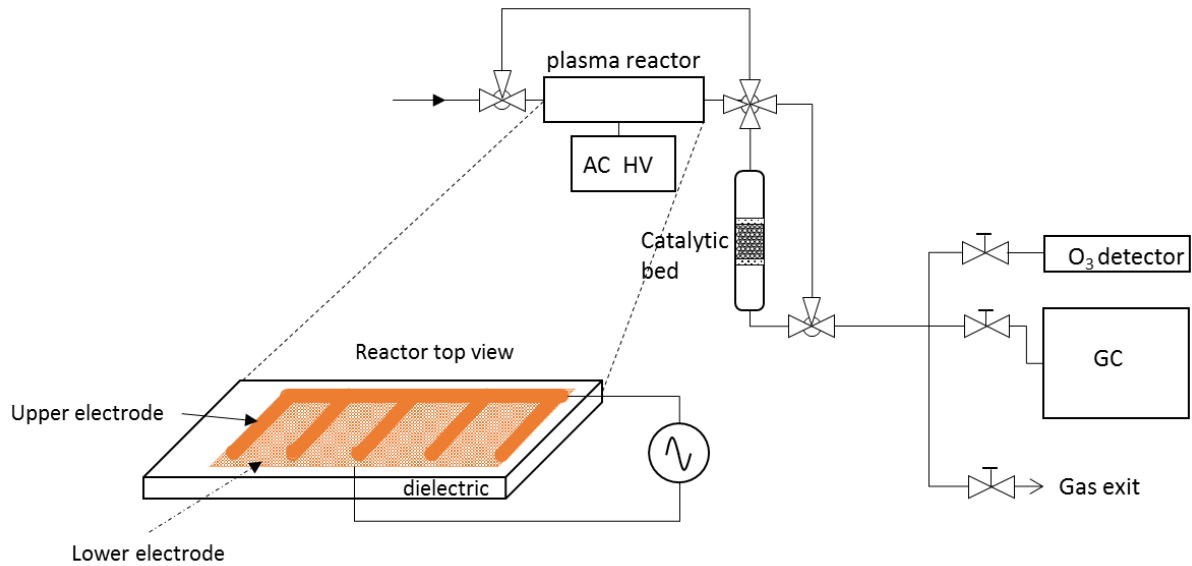
6 This work is in the continuity of a study started on methanol elimination by non thermal
7 plasma combined to catalysis at atmospheric pressure, in dry air conditions [22]. The effect of
8 humidity on the methanol conversion, by products selectivities and ozone concentration is
9 investigated. A high level of relative humidity is chosen, 35 % as it is representative of indoor
10 air levels. The plasma reactor was then associated to MnO_2 and CuO/MnO_2 based catalysts
11 placed in post discharge and the effect of the catalyst metal oxide ratio, preparation method
12 and methanol initial concentration were evaluated.

13 2. Experimental

14 2.1. Plasma reactor configuration

15 The NTAP reactor consisted in a surface dielectric barrier discharge (DBD) reactor. Two
16 electrodes (one copper comb and one copper plate stuck on the glass plate) were separated
17 from each other by a 2 mm thick glass plate acting as a dielectric barrier. Details of the reactor
18 and experimental setup can be found in [22]. 4g of catalyst were placed in the post discharge
19 (PP) area in a 1.6 cm inner diameter glass tube. The space occupied by the catalyst was 4.1
20 cm which corresponded to a residence time in the catalytic reactor of 100 ms. The NTAP
21 feeding gas was provided by an evaporating system (Serv'Instrumentation) with controlled
22 pollutant concentrations. The gas flow rate was kept constant ($5 \text{ L}\cdot\text{min}^{-1}$, residence time in
23 plasma alone: 0.36 s), whereas the methanol concentration could be varied from 25 to 200
24 ppmv. The presence of a manometer on the set-up allowed the control of the pressure drop.

1 Thanks to the structure of the catalyst support, consisting of alumina balls of 2 mm diameter,
2 the system remained at atmospheric pressure. The water vapor was controlled by a humidity
3 transmitter (Vaisala HTM330) with a constant content of 35 % RH which roughly
4 corresponded to 8050 ppmv at 20°C.



5
6 Figure 1: Experimental set-up.

7 2.2. Catalyst preparation

8 The section detailing the catalyst preparation can be found in [22]. Briefly, a solution of
9 $\text{Mn}(\text{NO}_3)_2 \cdot 4\text{H}_2\text{O}$ was mixed with 2 mm alumina balls and stirred for 4 hours in a rotary
10 evaporator under reduced pressure. The catalyst was dried at 110 °C and calcined at 300 °C.
11 The volume of precursor salt solution and weight of alumina were adjusted for a metal
12 loading of 5 wt. %.

13 The mixed oxides of CuO/MnO_2 were prepared by successive impregnation of alumina balls
14 by Mn or Cu nitrate solutions, separated by drying at 110 °C and calcinations at 300 °C as
15 previously described for single metal oxide catalyst. Two procedures have been used
16 according to the order of processing (copper first or manganese first). Metal content and
17 catalysts characterizations are gathered in Table 1.

1 Table 1: Metal oxide content (theoretical and measured from ICP¹), BET¹, support nature and
 2 preparation methods of the catalysts.

Catalyst name*	CuO content (wt. %)	MnO₂ content (wt. %)	S_{BET} (m².g⁻¹)	ICP (oxide wt.%)
Mn/Al	0	5	179	5.0
Cu/Al	5	0	197	3.9
SI-5Cu-5Mn	5	5	186	3.7 CuO 4.0 MnO ₂
SI-5Mn-5Cu	5	5	187	4.0 CuO 4.2 MnO ₂
CI-5Cu5Mn	5	5	191	3.7 CuO 4.2 MnO ₂
SI-25Cu-75Mn	2.5	7.5	186	2.5 CuO 7.4 MnO ₂
SI-75Cu-25Mn	7.5	2.5	194	7.6 CuO 2.5 MnO ₂

3 *SI: successive impregnation; CI: co-impregnation. The metal is cited in the order of
 4 impregnation. For example, Si-5Cu-5Mn corresponds to a catalyst prepared by successive
 5 impregnation of copper followed by manganese.¹Explained in the following section

6

7 2.3. Analytical methods

8 The energy density of the discharge was set at 20 J.L⁻¹ and its calculation is issued from the
 9 Manley method [23]. This method has been used in many reported studies. It links the voltage
 10 between the electrodes, ΔU , to the charge Q (measured via a capacitor placed in series) of the
 11 system. The plot of these series of data results in the so-called Lissajous curve whose
 12 integration leads to the energy per cycle (E_c) transferred through the gas. The discharge power
 13 (P) is obtained by multiplying the frequency (f) to the energy E_c . Dividing the power (P) by
 14 the gas flow rate (Q) results in the energy density, E_d (equation 1), which is a recurrent
 15 measure to compare plasma processes [22, 24].

1
$$E_d (J.L^{-1}) = \frac{P (Watt)}{Q (L.s^{-1})}$$

2 The specific surface area of the samples was measured by the Brunauer–Emmett–Teller
3 (BET) method after calcination of the catalyst at 400 °C. The metal loading was measured by
4 inductively coupled plasma optical emission spectrometry (ICP-OES). The catalysts were also
5 characterized by hydrogen temperature programmed reduction (H₂-TPR) [22].

6 Methanol conversion, X (%) and by-products selectivities, S (%) were calculated as follow:

7
$$X(\%) = \frac{[X]_0 - [X]}{[X]_0}$$

8 with [X]₀ = input methanol concentration and [X] = output methanol concentration

9

10
$$S_x(\%) = \frac{[R].(\text{number of Carbon of R})}{[X]_0 - [X]} \times 100$$

11 with [R] output concentration of product R

12 All the experiments were repeated 3 times and standard deviation of ±2 % was estimated. An
13 ozone analyzer (ES, Dualbeam 205) allowed the online measurement of the ozone upstream
14 and downstream the catalyst bed.

15 X-Ray diffraction patterns were obtained from a Siemens D5005 diffractometer using the
16 K_{Cuα1} = 1.5406 Å. The 2θ data within the 0° and 90° with a step size of 0.08° and an
17 integration time of 90s per step. Unfortunately, the structural characterization by XRD was
18 not usable. XRD diffraction lines of the catalysts show only alumina lines suggesting that
19 either the amount of oxides is too low to obtain a visible diffraction pattern or the oxides are
20 mainly amorphous.

21

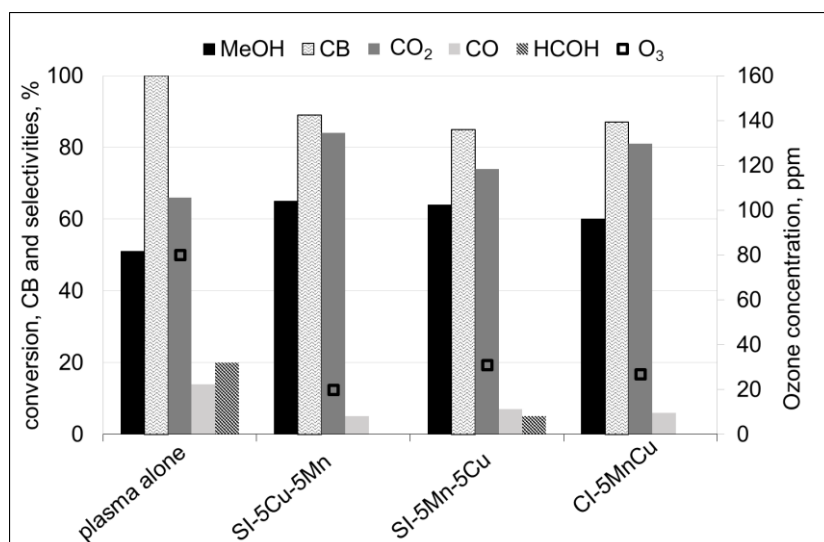
22

3. Results and discussion

3.1. Influence of the impregnation method

In order to select the best way to prepare the catalysts, the RE for methanol elimination of the different catalysts, in presence of humidity, were compared. The results are shown in Figures 2 and 3. The successive Cu/Mn impregnations procedure with, in first, copper impregnation seems to lead to better performances than the reverse (Figure 2). The SI-5Cu-5Mn catalyst appears to be slightly more efficient in carbon balance recovery, methanol conversion, ozone residual concentration and CO₂ selectivity than the corresponding catalyst SI-5Mn-5Cu prepared by manganese firstly impregnated, which leads also to formaldehyde.

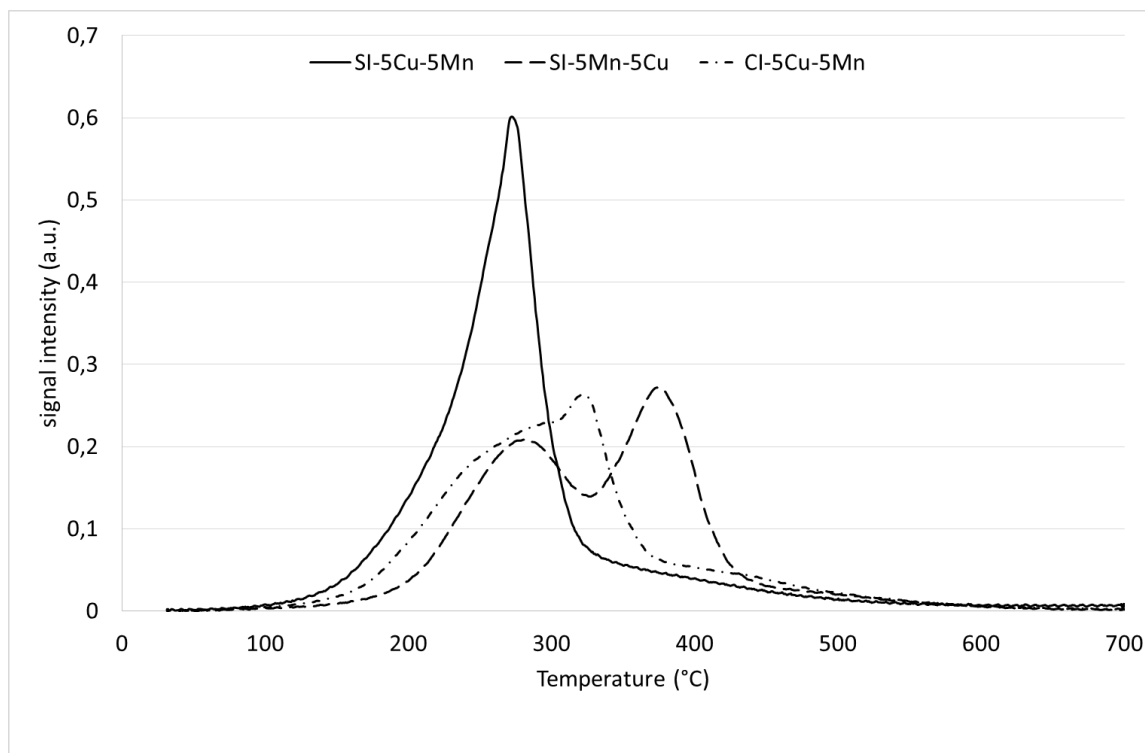
10



11

12 Figure 2: Effect of impregnation method of CuO/MnOx catalysts in post plasma configuration
13 on methanol conversion, carbon balance, ozone concentration and selectivities to secondary
14 products. Conditions: 20 J.L⁻¹, 50 ppm methanol, 35 % RH.

15 The oxidation state of manganese cations were characterized by temperature programmed
16 reduction (Figure 3). The TPR profile of the sample prepared by copper first impregnation
17 shows a single reduction peak centered at 250-280 °C, whereas the sample prepared by
18 manganese first impregnation shows two reduction peaks at 250-300°C and 350-380 °C.



1
2 Figure 3 : TPR profiles of the catalysts with different impregnation methods: SI-5Cu-5Mn,
3 SI-5Mn-5Cu and CI-5Cu-5Mn.

4 According to the total H₂ uptake experimental values, it is possible to estimate the respective
5 percentages of Mn^{IV} and Mn^{III} for each sample by assuming the total reduction of copper (Cu^{II}O
6 + H₂ → Cu⁰ + H₂O) and the reduction of manganese species to Mn^{II} (Mn^{IV}O₂ + H₂ → Mn^{II}O +
7 H₂O and Mn^{III}O_{1.5} + 1/2H₂ → Mn^{II}O + 1/2H₂O). The results are gathered in Table 2.

8

9 Table 2: Hydrogen consumption for the oxide reduction (cm³ H₂/g ± 5 %) STP.

	SI-25Cu- 75Mn	SI- 5Cu- 5Mn	SI-75Cu- 25Mn	SI-5Mn-5Cu	CI-5Cu5Mn	Mn/Al
Mn (wt%)	4.7	2.5	1.6	2.7	2.7	3.2
Cu (wt%)	2.0	3.0	6.1	3.2	3.0	0

$V_{\text{exp}}(\text{cm}^3\text{H}_2/\text{g})$	19.1	18.7	29.6	23.8	19.8	13.7
%Mn ^{IV}	13	37	93	100	49	99
%Mn ^{III}	87	63	7	≈0	51	1
Cu/Mn at. ratio	0.37	1.04	3.3	1.02	0.96	-

1

2 It appears that the sample prepared by manganese first impregnation contains only Mn^{IV},

3 whereas the sample prepared by copper impregnation first contains mainly Mn^{III}. The two peaks

4 profile of SI-5Mn-5Cu sample could then be explained by the reduction of Cu^{II} to Cu⁰ and Mn^{IV}

5 to Mn^{III} for the peak at the lowest temperature and to the reduction of Mn^{III} to Mn^{II} for the

6 highest one. The reduction profile of the SI-5Cu-5Mn sample which presents a single peak at

7 low temperature could suggest that a strong interaction exists between copper and manganese

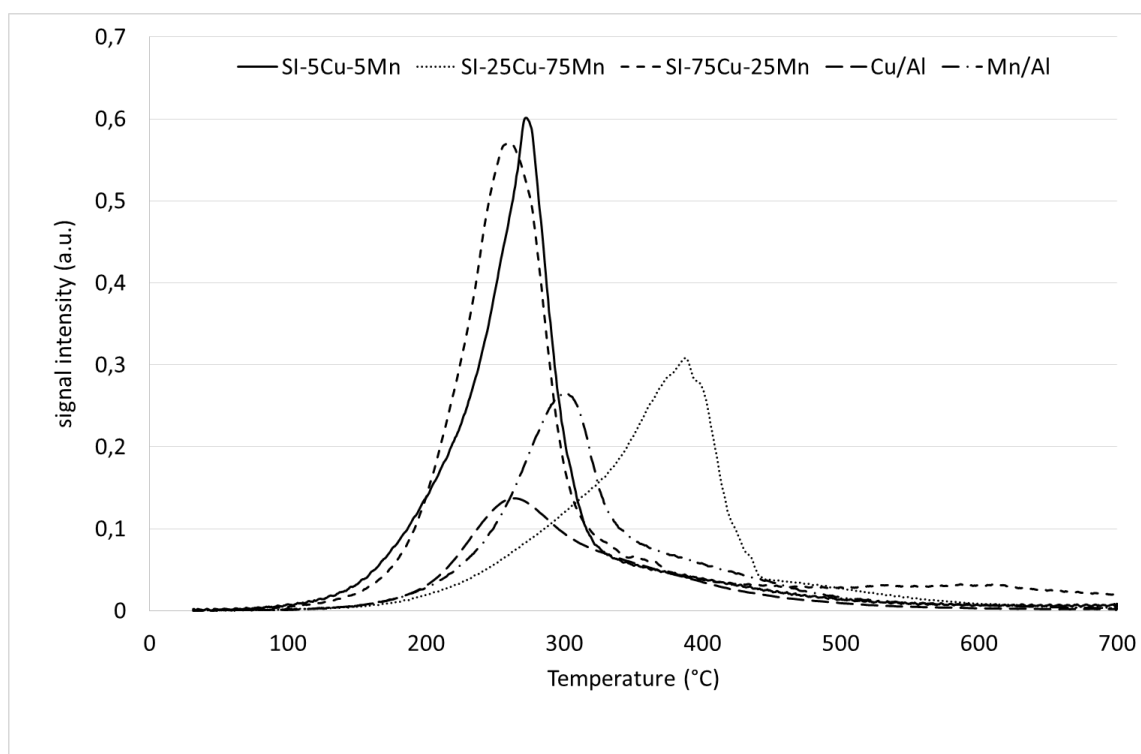
8 increasing the reducibility of Mn^{III} [25].

9 By varying the Cu/Mn atomic ratio, it appears that the percentage of Mn^{IV} increases with the

10 copper content for the samples prepared by successive impregnation with copper first.

11 The TPR profiles of the samples prepared by copper first impregnation are shown on Figure 4

12 along with profiles of manganese and copper oxides alone.

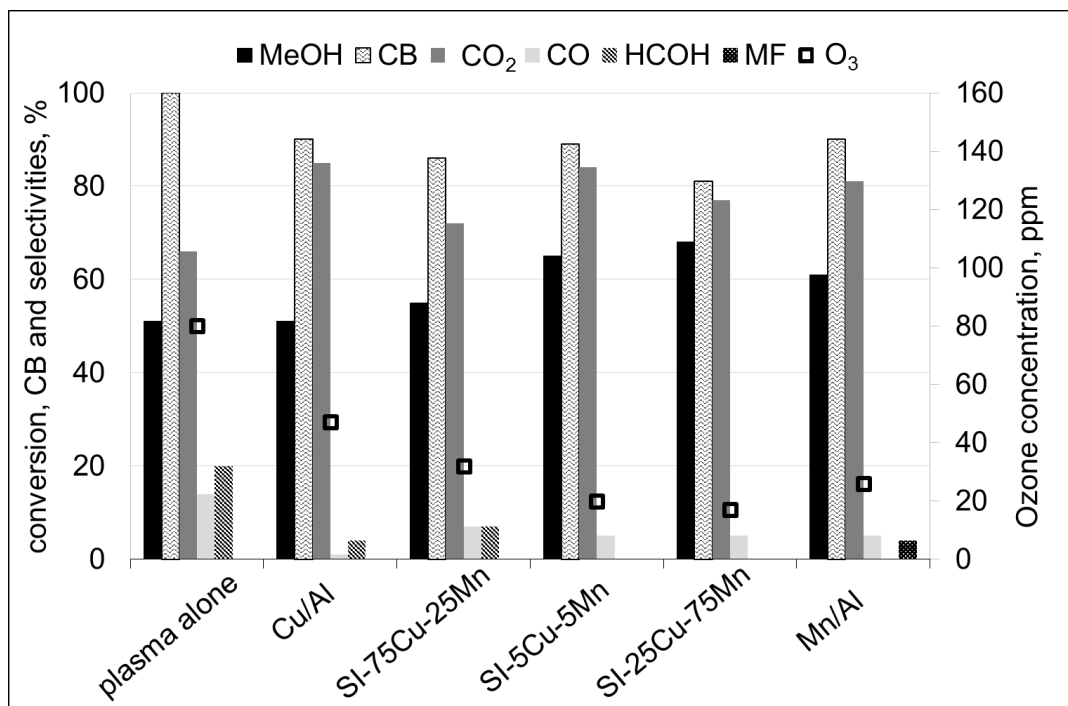


1
 2 Figure 4: TPR profiles of the catalysts with different oxide ratios: SI-5Cu-5Mn, SI-25Cu-
 3 75Mn, SI-75Cu-25Mn, Mn/Al and Cu/Al.

4
 5 For the Cu/Mn atomic ratio higher than 1, the reduction behavior is similar to single oxides,
 6 with the presence of only one reduction peak at low temperature. However, for the lowest ratio
 7 (Cu/Mn = 0.37) a single peak is also observed but at higher temperature (380-400°C) and could
 8 indicate the formation of a defined compound more stable than single oxides of copper and
 9 manganese. This compound could be a copper manganese spinel (CuMn_2O_4) for the lowest
 10 Cu/Mn atomic ratio which is destabilized when the copper content increases [26]. The MnO_2
 11 catalyst (Mn/Al) profile (Figure 4), as described in our previous publication, shows a main
 12 reduction peak at 300°C and a small shoulder between 350-480°C, resulting from the reduction
 13 of MnO_2 to $\text{Mn}_2\text{O}_3/\text{Mn}_3\text{O}_4$ then MnO [27] or from the reduction of Mn_5O_8 to Mn_3O_4 then MnO
 14 as observed by Ye and al. [25].
 15 It was demonstrated that copper addition tends to maintain MnO_2 oxide phase, while higher
 16 manganese oxide content leads to Mn_2O_3 phase, hindering the copper oxide effect [28].

1 It was suggested, in the case of mixed oxides, that the activity depends on the redox couple
2 $\text{Mn}^{3+} + \text{Cu}^{2+} \leftrightarrow \text{Mn}^{4+} + \text{Cu}^{+}$ [29] which could be present on manganese copper spinel structure
3 (Mn^{3+} oxidation state). We can expect that the highest interactions between copper and
4 manganese cations lead to the highest catalytic activity, as observed for the SI-5Cu-5Mn and
5 SI-25Cu-75Mn catalysts. To notice, these samples contain mainly manganese as Mn^{III} (Table
6 2). The MnO_2 catalyst (Mn/Al) profile (Figure 4), as described in our previous publication,
7 shows a main reduction peak at 300°C and a small shoulder between 350-480°C, resulting from
8 the reduction of MnO_2 to $\text{Mn}_2\text{O}_3/\text{Mn}_3\text{O}_4$ then MnO [27] or from the reduction of Mn_5O_8 to
9 Mn_3O_4 then MnO as observed by Ye and al. [25].

10 The percentage of loaded metal oxide was also evaluated in terms of methanol RE (Figure 5).
11 It appeared that the ozone degradation is dependent on the percentage of loaded manganese
12 resulting in only 17 ppm left after one passage over SI-25Cu-75Mn, while it remains at
13 32ppm over SI-75Cu-25Mn. Methanol conversion increases as a function of ozone
14 degradation, indicating a reaction in which the plasma oxidizing species (O^{\bullet} , OH^{\bullet} , HO_2^{\bullet}) are
15 given first place for methanol conversion. As specified above, Cu/Mn redox couple and MnO_2
16 phase availability are responsible of ozone degradation into oxidizing species. Only little
17 effect is observed on the carbon balance between the different metal oxide ratios which
18 remains close to 90% except SI-25Cu-75Mn that drops at 80 %. The drop in carbon balance
19 could be related to formic acid formation.



1

2 Figure 5: Effect of metal oxide ratio of MnO₂/CuO catalysts placed in post plasma
 3 configuration on methanol conversion, ozone concentration and selectivities to secondary
 4 products: HCOH; MF: methyl formate. Conditions: 20J.L⁻¹, 50 ppm methanol, 35% humidity.

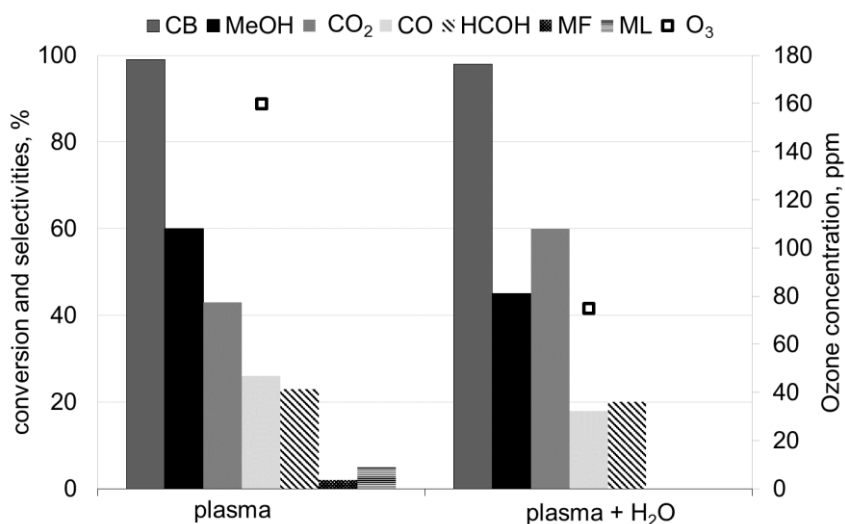
5 According to the fair methanol RE, carbon balance and selectivity to by-products (especially
 6 to CO₂), the catalyst prepared via successive impregnation with CuO first, SI-5Cu-5Mn, was
 7 chosen as reference catalyst and further investigated.

8

9 4. Influence of humidity

10 4.1. Effect of humidity in plasma alone configuration

11 The addition of 35 % relative humidity in the gas flow led to a decrease of the methanol
 12 conversion, from 60 % to 43% and ozone concentration (160 ppm to 75 ppm) but did not
 13 affect the carbon balance of the reaction which remained close to 100% (Figure 6).



1
 2 Figure 6: Effect of water on methanol conversion, ozone concentration and selectivities to
 3 secondary products: HCOH; ML: methylal; MF: methyl formate. Conditions: 20J.L⁻¹, 50 ppm
 4 methanol.

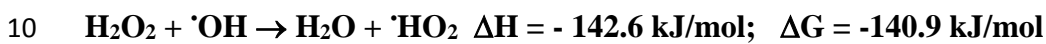
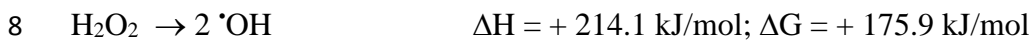
5 When looking at the by-products selectivities, the presence of humidity improves the
 6 selectivity of the reaction to carbon dioxide rather than CO, slightly affects formaldehyde
 7 (HCOH), while neither methyl formate (MF) nor methylal (M) are detected. These effects
 8 were observed by different authors [4–8, 10]. They have postulated that the presence of
 9 relatively low humidity levels increases the concentration of [•]OH radicals that can enhance
 10 the chemical reactivity. Concomitantly, the lower ozone production could be due to its
 11 reaction with H[•], [•]OH and [•]HO₂ arising from water dissociation and/or from the succession of
 12 reactions involving O and [•]OH. According to thermodynamic data (Ref. NIST), the reaction
 13 of H₂O with O radical leads to the formation of hydrogen peroxide rather than direct [•]OH
 14 radical formation since an estimation of the value of the variation of Gibbs energy at 300K
 15 (ΔG) shows that the only reaction between water and O with $\Delta G < 0$ is the formation of
 16 hydrogen peroxide (Table 3). Moreover, the further reactions between hydrogen peroxide and
 17 O or [•]OH radicals are thermodynamically favored and lead to the formation of [•]OH and [•]HO₂

1 which are highly oxidative species. It means that the $\cdot\text{OH}$ and $\cdot\text{HO}_2$ generation occurs most
 2 probably by hydrogen peroxide secondary reactions rather than by water dissociation or direct
 3 reaction of O radical with water.

4 Table 3: Thermodynamic data.

Product	ΔH°_f (kJ/mol)	S° 300K (J/mol.K)
H_2O_2	-136.1	239.9
H_2O	-241.8	188.8
$\cdot\text{HO}$	+39.0	183.7
$\cdot\text{HO}_2$	+2.1	229.1
O°	+249.2	161.1

5



11

12 Moreover, the VOC conversion and ozone concentration were reduced at high humidity levels
 13 (level depending on plasma discharge type) due to the modification of the discharge electric
 14 field, leading to a decrease of reactive plasma volume and chemical species [14]. Regarding
 15 by-products selectivity, the affinity of formaldehyde to water would favor its direct
 16 transformation into CO_2 at the expense of CO, according to Sugasawa [9]. The total oxidation
 17 of methyl formate and methylal under humid flow contributes to the improved CO_2
 18 selectivity.

19

1 4.2. Effect of humidity in presence of a post plasma (PP) catalyst

2 As already observed in our previous publication [22], and from the results cited above, a 5 %
3 $\text{MnO}_2/5\% \text{ CuO}/\text{Al}_2\text{O}_3$ catalyst presented some of the best activities, such as methanol
4 conversion or ozone degradation, that swayed our catalyst choice to SI-5Cu-5Mn in the study
5 of the humidity impact on methanol elimination efficiency. In order to evaluate the efficiency
6 in presence of a catalyst in post-plasma location, 4 g of SI-5Cu-5Mn catalyst were placed
7 immediately after the plasma reactor in a specific catalytic reactor.

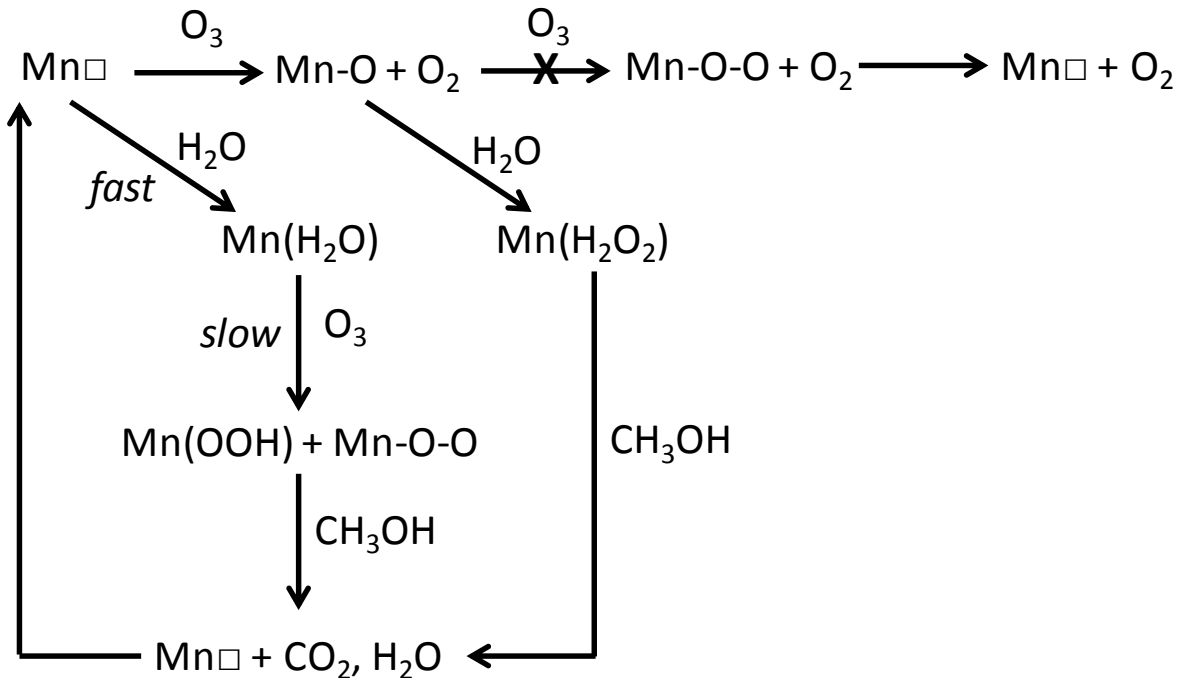
8 In dry conditions, when 4 g of catalyst were placed in post plasma, the methanol conversion
9 and carbon balance were close to 100 % with only formation of carbon oxides ($\text{CO} = 43\%$;
10 $\text{CO}_2 = 55\%$) for the plasma and catalyst reactors connected in series. In presence of humidity
11 ($\text{RH} = 35\%$ corresponding to about 8000 ppmv) a large decrease in conversion was observed.
12 The methanol total conversion decreased from 100 % to 65 % and the carbon balance from
13 99 % to 89 %, but the CO_2 selectivity increased to 83 %, with only 6 % of CO. The most
14 significant effect concerned ozone exiting the plasma reactor which decreased from 160 ppmv
15 in dry conditions to 74 ppmv under 35% of RH.

16 On the catalyst, the ozone consumption reached 148 ppmv in dry conditions (ozone
17 conversion=92.5%) and only 54 ppmv in presence of humidity (ozone conversion = 73 %).
18 The residual ozone concentration is higher in presence of humidity (20 ppmv) than in dry
19 conditions (12 ppmv) despite a lower initial concentration entering the catalyst reactor (75
20 ppm in humid vs 160 ppm in dry conditions). The results are gathered in Tables 4 and 5. On
21 the same tables, the calculation of conversions and selectivities are done according to the
22 consumption of methanol for the plasma reactor and to the sum of the consumptions of all the
23 products for the catalyst reactor, taking into account the carbon number for methyl formate
24 and methylal.

1 For example, in dry conditions (Table 4) the consumption of the products appears to be 20
2 ppm for methanol, 7 ppm for formaldehyde, 0.5 ppm for methyl formate (corrected to 1 ppm),
3 0.3 ppm for methylal (corrected to 0.9 ppm) and 0.1 ppm for formic acid, leading to a total
4 consumption of 29 ppm. The value of formic acid formation (formic acid is not detected but
5 its formation is expected according to the possible reaction of oxidation of methanol) is
6 estimated from the carbon balance defect. The CO₂ (50%) and CO (47%) selectivities are then
7 calculated as the ratio between their increased concentration through the catalyst reactor (14.5
8 ppm for CO₂ and 13.5 ppm for CO) and the sum of the products consumption (29 ppm).
9 According to our calculations it appears that the methanol conversion on the catalyst is higher
10 in dry (or pseudo-dry conditions since 51 ppm of water are produced in the plasma reactor
11 due to the methanol oxidation), than in humid conditions in presence of more than 8000 ppm
12 of water, but the selectivity to CO₂ is lower (50%) in dry conditions compared to 82% in
13 humid conditions without CO formation. In dry conditions, the selectivity to CO is 47%.
14 This surprising effect could be correlated with the possible mechanism of ozone and water
15 reaction on the manganese oxide surface. It is well admitted that ozone reacts with manganese
16 surface cations to form Mn-O⁺ or Mn-OO⁺ surface species [30]. In presence of water the
17 reaction of ozone on the catalyst surface was partly inhibited due to the water adsorption on
18 the manganese active sites [31, 32]. A mechanism was proposed by Zhu *et al.* [33] for the
19 reaction of ozone decomposition on manganese oxide in presence of gaseous water. It consists
20 of the slow reaction of ozone on adsorbed water leading to the formation, at the catalyst
21 surface, of hydroxyl species on which further ozone molecules can react to form
22 hydroperoxide species and peroxide species. Nevertheless, the possible formation of hydrogen
23 peroxide cannot be excluded from direct reaction between Mn-O species and water from the
24 gas phase leading to the formation of surface hydroxyl species on which ozone can react [33]

1 (Scheme 1) blocking partially the ozone elimination cycle, but allowing the formation of the
 2 highly oxidative hydroperoxide species.

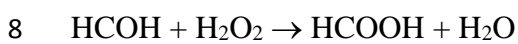
3



4

5 Scheme 1: Pathway of ozone elimination in presence of water [33]

6 According to this hypothesis, the formic acid formation estimated from the carbon balance
 7 defect could result from formaldehyde oxidation by H_2O_2 or $\cdot\text{OH}$ [17]:



10

11

12

13

14

15

1 Table 4: Dry conditions: Summary of the methanol conversion and products selectivity on
 2 plasma and catalyst reactors and products concentration after plasma and catalyst reactors. “S
 3 product”: selectivity to products. (Experimental conditions: 20 J.L⁻¹, catalyst = 4 g, total flow
 4 rate = 5 L.min⁻¹).

Plasma reactor (P)		Catalyst (C)		Total (P+C)		
Products	Initial (ppm)	CH ₃ OH conv S products (%)	[Product] (ppm)	CH ₃ OH conv S products (%)	[Product] (ppm)	CH ₃ OH & O ₃ conv. (%) S products (%)
CH ₃ OH	50	60	20	100	0	100
CO ₂	0	43	13	50	27.5	55
CO	0	27	8	47	21.5	43
HCOH	0	23	7	0	0	0
MF	0	3	0.5	0	0	0
ML	0	3	0.3	0	0	0
<i>HCOOH</i> *	0	≈ 0	0.1	3	1.0	2
H ₂ O	0	-	51	-	99	-
O ₃	0	-	160	-	12	92.5

5 *estimated values calculated from the carbon balance defect

6

7 Table 5: Humid conditions: Summary of the methanol conversion and products selectivity on
 8 plasma and catalyst reactors and products concentration after plasma and catalyst reactors.
 9 (Experimental conditions: 20 J.L⁻¹, catalyst = 4 g, total flow rate = 5 L.min⁻¹).

Plasma reactor (P)		Catalyst (C)		Total (P+C)		
Products	Initial (ppm)	CH ₃ OH conv S products (%)	[Product] (ppm)	CH ₃ OH conv S products (%)	[Product] (ppm)	CH ₃ OH & O ₃ conv. (%) S products (%)
CH ₃ OH	50	45	27.5	36	17.5	65
CO ₂	0	60	13.5	82	27	83

CO	0	18	4	0	2	6
HCOH	0	20	4.5	0	0	0
MF	0	0	0	0	0	0
ML	0	0	0	0	0	0
<i>HCOOH</i> *	0	2	0.5	18	3.5	11
H ₂ O	>8000	-	>8000	-	>8000	-
O ₃	0	-	74	-	20	73

1 *estimated values calculated from the carbon balance defect

2

3 4.3. Reactivity as a function of methanol concentration in humid reaction conditions

4 We have already shown [22] that in dry reaction conditions, a strong influence on reaction

5 behavior occurs when the initial methanol concentrations change. The influence of humidity

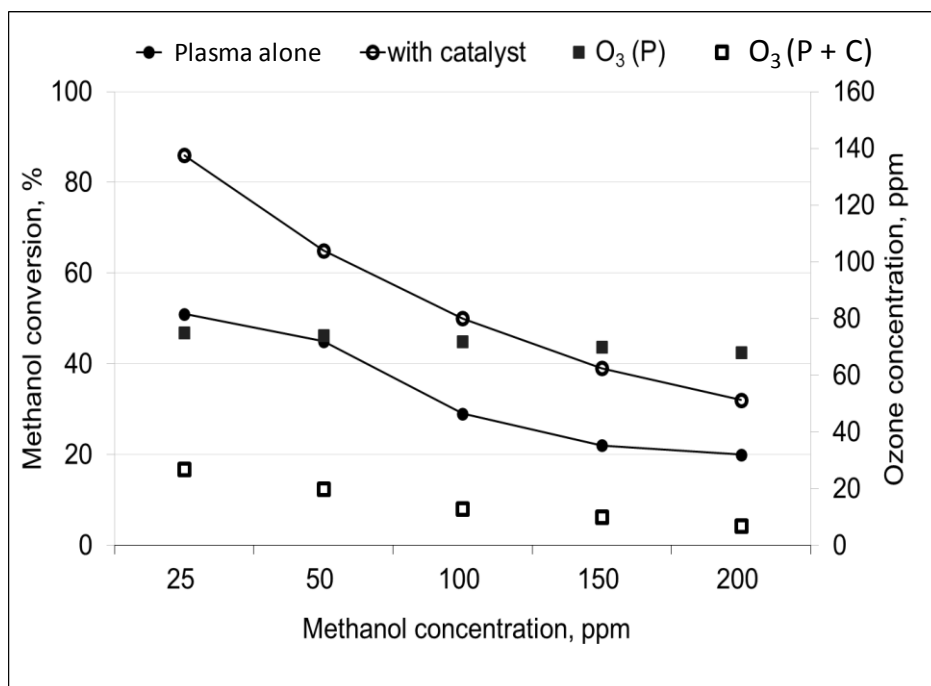
6 (RH = 35 %) on the reaction behavior was evaluated as a function of initial methanol

7 concentration, both in plasma alone and with the catalytic reactor. The methanol initial

8 concentration was varied from 25 to 200 ppmv and in post plasma catalytic configuration, 4 g

9 of the reference catalyst SI-5Cu-5Mn was used.

10 The results are gathered in Figures 7, 8 and on Tables 6 and 7.



1

2 Figure 7: Effect of methanol initial concentration on methanol conversion and ozone
 3 concentration in single plasma and with 4g of SI5Cu-5Mn catalyst in post plasma.

4

5 Table 6: Methanol conversion and concentration after plasma alone (P), plasma + catalyst (P
 6 + C) and catalyst alone (C) with ozone consumption (experimental and calculated from
 7 observed products formation).

[MeOH] ^o (ppmv)	[MeOH] After plasma (ppmv)	MeOH transformed by plasma (ppmv)	[MeOH] After catalyst (ppmv)	MeOH transformed (P + C) (ppmv)	Conv. MeOH (P) (%)	Conv. MeOH (C) (%)	Conv. MeOH (P+C) (%)	[O ₃] ^o After plasma (ppmv)	[O ₃] After catalyst (ppmv)	O ₃ (exp.) consumption (ppmv)	O ₃ (th.) consumption on catalyst (ppmv)
(1)	(2)	(3)	(4)	(5)	(6)	(7)	(8)	(9)	(10)	(11)	(12)
25	12.3	12.7	3.5	21.5	51	71	86	75	27	48	31
50	27.5	22.5	17.5	32.5	45	36	65	74	20	54	39
100	71	29	50	50	29	30	50	72	13	59	68
150	117	33	91.5	58.5	22	22	39	70	10	60	70
200	160	40	136	64	20	15	32	68	7	61	67

8

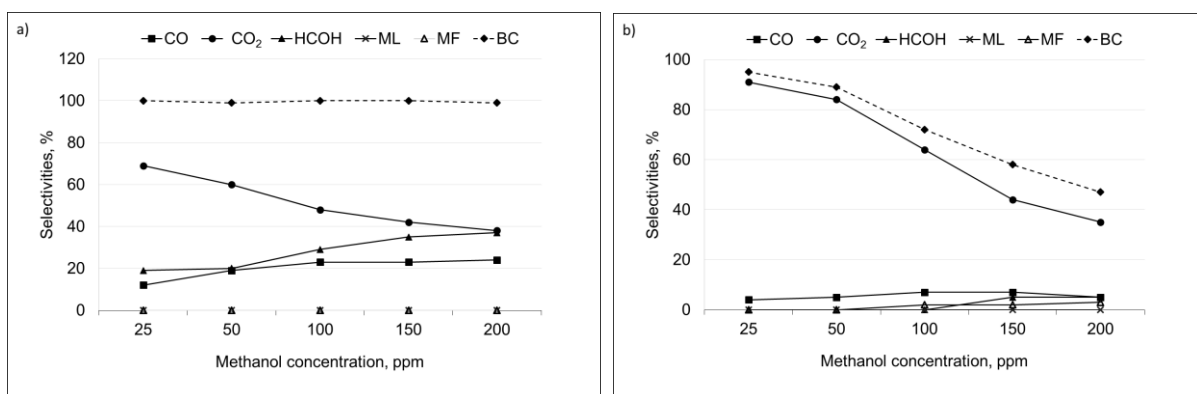
9

10

1 Table 7: Methanol and products transformation on the catalyst SI-5Cu-5Mn as a function of the
 2 methanol concentration at the entrance of the catalytic reactor.

(1) MeOH at the entrance of the catalyst (ppmv)	(2) MeOH transformed on the catalyst (ppmv)	(3) CO ₂ formation on the catalyst (ppmv)	(4) CO transformed on the catalyst (ppmv)	(5) CO ₂ from total oxidation of MeOH and HCOH (ppmv)	(6) HCOH transformed on the catalyst (ppmv)	(7) Selectivity to CO ₂ for MeOH and HCOH oxidation (%)	(8) Carbon balance defect (ppmv)	(9) Ratio $\frac{[O_3]^0}{([MeOH]+[HCOH])}$
12.3	8.8	10.8	0.7	10.1	2.4	90	1.1	5.1
27.5	10.0	13.8	2.7	11.1	4.5	77	3.6	2.3
71	21.0	18.1	3.2	14.9	8.4	51	14.0	0.9
117	25.5	11.9	3.5	8.4	8.6	25	24.6	0.5
160	24.0	7.2	6.4	0.8	11.6	2	33.9	0.4

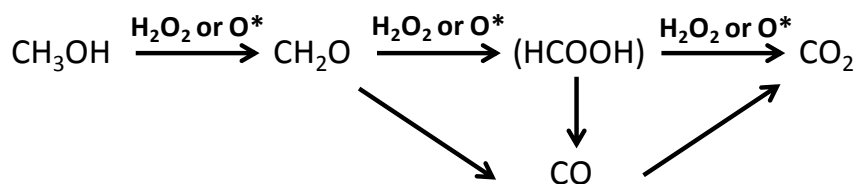
3
 4 In plasma alone and at constant input specific energy (20 J.L⁻¹) the methanol conversion
 5 decreases with the increase of initial concentration, as already observed. Nevertheless the total
 6 amount of methanol transformed increases with the methanol initial concentration and the
 7 formaldehyde formation increases to the detriment of CO₂ formation (Figure 8).



13 Figure 8: Effect of methanol initial concentration on carbon balance and selectivities to
 14 secondary products: CO, CO₂, HCOH; ML: methylal; MF: methyl formate a) in plasma alone
 15 and b) with 4g of SI-5Cu-5Mn in post plasma. Conditions: 20J.L⁻¹, 35% humidity.

16
 17 On the catalyst, the amount of methanol transformed (Table 7 (2)) increases with the
 18 concentration of methanol at the entrance of catalyst reactor and seems to reach a plateau for

1 a concentration higher than 71 ppmv, similarly to ozone consumption (Table 6 (11)).
 2 Regarding the CO₂ formation (Table 7 (3)), it goes through a maximum and then decreases
 3 for methanol initial concentration higher than 71 ppmv. From the data collected at the
 4 entrance and at the exit of the catalytic reactor, it is possible to estimate the amount of the
 5 products (CO and HCOH) transformed on the catalyst. Additionally, it is possible to estimate
 6 the concentration of CO₂ formed on the catalyst coming from methanol and formaldehyde
 7 total oxidation. The results obtained by subtracting the CO transformed on the catalyst (the
 8 only oxidation product of CO being CO₂) to the CO₂ formed on the catalyst (column (3) –
 9 column (4)) are plotted on column (5) of the Table 7. It shows that the amount of CO₂ from
 10 the total oxidation of methanol and formaldehyde (VOC products) depends of the ratio
 11 between VOC products and ozone (Table 7 column (9)). The selectivity to CO₂ from total
 12 oxidation of methanol and formaldehyde decreases from 90% to only 2% when the ratio
 13 between VOC and ozone decreases from 5.1 to 0.4. Simultaneously, the carbon balance
 14 defect (Table 7 (8)), which indicates the formation of undetected product, expected to be
 15 formic acid, [34, 35], increases from 1.1 to 33.9 ppmv. This behavior is consistent with the
 16 usual reaction mechanism of partial methanol oxidation involving successive reaction [34,
 17 35]:



19

20 Scheme 1: Partial oxidation of methanol.

21

22 In dry conditions, the higher ozone concentration on the catalyst could favor the
 23 formaldehyde and formic acid oxidation to carbon oxides, whereas in presence of water,

1 either the lower ozone concentration or the presence of hydrogen peroxide resulting of the
2 reaction of activated oxygen species from ozone with water could favor the formation of
3 formic acid instead of the total oxidation of formaldehyde.

4

5 5. Conclusion

6 Under humid conditions (37 % RH), close to ambient air concentrations, and at low energy
7 density (20J.L^{-1}), non thermal plasma treatment of methanol affects the conversion rate
8 compared to dry air but improves largely the CO_2 selectivity in presence of a CuO-MnO_2
9 based catalyst in post plasma configuration. Additionally, selectivities to secondary products
10 are reduced (CO and HCOH) and no methylal, nor methyl formate are yielded at low
11 concentrations ($\leq 50\text{ppm}$). The presence of humidity in the discharge leads to a reduction of
12 ozone concentration which contribute to the partial methanol oxidation. These results could be
13 explained by a reaction between ozone and adsorbed water leading to the formation of
14 hydroperoxide species and/or adsorbed H_2O_2 more selective to CO_2 formation. The presence
15 of these species and a low O_3 concentration would favor the formation of formic acid instead
16 of the total oxidation of formaldehyde to CO_2 . We could also expect that these reactions block
17 partially the cycle of ozone decomposition, therefore explaining the leftover ozone detected at
18 the exit of the plasma catalyst reactor. The impregnation method and metal oxide ratios
19 showed a little effect on the conversion rate of methanol, a 5 % MnO_2 / 5 % $\text{CuO} / \text{Al}_2\text{O}_3$
20 catalyst prepared by successive impregnations results in the best conversion rates and CO_2
21 selectivity.

22

23 Acknowledgment

24 The authors are thankful to the ANRT for the financial support.

1 References

2 [1] A.M. Vandenbroucke, R. Morent, N. De Geyter, C. Leys, Non-thermal plasmas for
3 non-catalytic and catalytic VOC abatement, *J Hazard Mater.* 195 (2011) 30-54

4 [2] G. Xiao, W. Xu, R. Wu, M. Ni, C. Du, X. Gao, Z. Luo, K. Cen, Non-Thermal Plasmas
5 for VOCs Abatement, *Plasma Chem Plasma Process*, 34 (2014) 1033–1065

6 [3] M. Schiavon, V. Torretta, A. Casazza, M. Ragazzi, Non-thermal Plasma as an
7 Innovative Option for the Abatement of Volatile Organic Compounds: a Review, *Water*
8 *Air Soil Pollut.* 228 (2017) 388-408

9 [4] J. Van Durme, J. Dewulf, W. Sysmans, C. Leys, H. Van Langenhove, Abatement and
10 degradation pathways of toluene in indoor air by positive corona discharge, *Chemosphere.*
11 68 (2007) 1821–1829

12 [5] J. Van Durme, J. Dewulf, W. Sysmans, C. Leys, H. Van Langenhove, Efficient
13 toluene abatement in indoor air by a plasma catalytic hybrid system, *Appl. Catal. B*
14 *Environ.* 74 (2007) 161–169.

15 [6] A.M. Vandenbroucke, M.T. Nguyen Dinh, N. Nuns, J.-M. Giraudon, N. De Geyter, C.
16 Leys, J.-F. Lamonier, R. Morent, Combination of non-thermal plasma and Pd/LaMnO₃
17 for dilute trichloroethylene abatement, *Chem. Eng. J.* 283 (2016) 668–675

18 [7] O. Karatum, M.A. Deshusses, A comparative study of dilute VOCs treatment in a non-
19 thermal plasma reactor, *Chem. Eng. J.* 294 (2016) 308–315

20 [8] L. Sivachandiran, F. Thevenet, P. Gravejat, A. Rousseau, Isopropanol saturated TiO₂
21 surface regeneration by non-thermal plasma: Influence of air relative humidity, *Chem.*
22 *Eng. J.* 214 (2013) 17–26

- 1 [9] M. Sugasawa, T. Terasawa, S. Futamura, Additive Effect of Water on the
2 Decomposition of VOCs in Nonthermal Plasma, *IEEE Trans. Ind. Appl.* 46 (2010) 1692–
3 1698.
- 4 [10] J. Van Durme, J. Dewulf, K. Demeestere, C. Leys, H. Van Langenhove, Post-plasma
5 catalytic technology for the removal of toluene from indoor air: Effect of humidity, *Appl.*
6 *Catal. B Environ.* 87 (2009) 78–83
- 7 [11] S. Futamura, M. Sugasawa, Additive Effect on Energy Efficiency and Byproduct
8 Distribution in VOC Decomposition with Nonthermal Plasma, *IEEE Trans. Ind. Appl.* 44
9 (2008) 40–45.
- 10 [12] E.H. Lock, A.V. Saveliev, L.A. Kennedy, Methanol and Dimethyl Sulfide Removal
11 by Pulsed Corona Part I: Experiment, *Plasma Chem. Plasma Process.* 26 (2006) 527–542
- 12 [13] G. Yu-fang, Y. Dai-qi, T. Ya-feng, C. Ke-fu, Humidity Effect on Toluene
13 Decomposition in a Wire-plate Dielectric Barrier Discharge Reactor, *Plasma Chem.*
14 *Plasma Process.* 26 (2006) 237–249.
- 15 [14] Z. Falkenstein, J.J. Coogan, Microdischarge behaviour in the silent discharge of
16 nitrogen-oxygen and water-air mixtures, *J. Phys. Appl. Phys.* 30 (1997) 817.
- 17 [15] R. Ono, T. Oda, Measurement of hydroxyl radicals in pulsed corona discharge,
18 *J. Electrostat.* 55 (2002) 333–342.
- 19 [16] L. Fouad, S. Elhazek, Effect of humidity on positive corona discharge in a three
20 electrode system, *J. Electrostat.* 35 (1995) 21–30.
- 21 [17] S. Lovascio, N. Blin-Simiand, L. Magne, F. Jorand, S. Pasquiers, Experimental Study
22 and Kinetic Modeling for Ethanol Treatment by Air Dielectric Barrier Discharges, *Plasma*
23 *Chem Plasma Process.* 35 (2015) 279-301

- 1 [18] T. Zhu, J. Li, Y. Jin, Y. Liang, G. Ma, Decomposition of benzene by non-thermal
2 plasma processing: Photocatalyst and ozone effect, *Int. J. Environ. Sci. Technol.* 5 (2008)
3 375–384.
- 4 [19] M.T.N. Dinh, J.-M. Giraudon, J.-F. Lamonier, A. Vandenbroucke, N. De Geyter, C.
5 Leys, R. Morent, Plasma-catalysis of low TCE concentration in air using $\text{LaMnO}_{3+\delta}$ as
6 catalyst, *Appl. Catal. B Environ.* 147 (2014) 904–911
- 7 [20] H. Einaga, M. Harada, S. Futamura, Structural changes in alumina-supported
8 manganese oxides during ozone decomposition, *Chem. Phys. Lett.* 408 (2005) 377–380.
- 9 [21] B.-D. Yan, S. Meilink, G. Warren, P. Wynblatt, Water Adsorption and Surface
10 Conductivity Measurements on alpha Alumina Substrates, *IEEE Trans. Compon. Hybrids*
11 *Manuf. Technol.* 10 (1987) 247–251.
- 12 [22] C. Norsic, J.-M. Tatibouët, C. Batiot-Dupeyrat, E. Fourré, Non thermal plasma
13 assisted catalysis of methanol oxidation on Mn, Ce and Cu oxides supported on $\gamma\text{-Al}_2\text{O}_3$,
14 *Chem. Eng. J.*, 304 (2016) 563-572
- 15 [23] T.C. Manley, The Electric Characteristics of the Ozonator Discharge, *Trans.*
16 *Electrochem. Soc.* 84 (1943) 83–96
- 17 [24] I. Biganzoli, R. Barni, A. Gurioli, R. Pertile, C. Riccardi, Experimental investigation
18 of Lissajous figure shapes in planar and surface dielectric barrier discharges, *J. Phys.*
19 *Conf. Ser.* 550 (2014) 12039
- 20 [25] Z. Ye, J.-M. Giraudon, N. Nuns, P. Simon, N. De Geyter, R. Morent, J.-F. Lamonier,
21 Influence of the preparation method on the activity of copper-manganese oxides for
22 toluene total oxidation, *Appl. Cat. B: Env.* 223 (2018) 154–166

- 1 [26] I. Spassova, M. Khristova, D. Panayotov, D. Mehandjiev, Coprecipitated CuO–
2 MnO_x Catalysts for Low-Temperature CO–NO and CO–NO–O₂ Reactions, *J. Catal.* 185
3 (1999) 43–57
- 4 [27] J. Jarrige, P. Vervisch, Plasma-enhanced catalysis of propane and isopropyl alcohol
5 at ambient temperature on a MnO₂-based catalyst, *Appl. Cat B: Environ.* 90 (2009) 74–82
- 6 [28] S.M. Saqer, D.I. Kondarides, X.E. Verykios, Catalytic oxidation of toluene over
7 binary mixtures of copper, manganese and cerium oxides supported on γ -Al₂O₃, *Appl.*
8 *Catal. B Environ.* 103 (2011) 275–286
- 9 [29] K. Qian, Z. Qian, Q. Hua, Z. Jiang, W. Huang, Structure–activity relationship of
10 CuO/MnO₂ catalysts in CO oxidation, *Appl. Surf. Sci.* 273 (2013) 357–363
- 11 [30] W. Li, G. V. Gibbs, S. T. Oyama, Mechanism of Ozone Decomposition on a
12 Manganese Oxide Catalyst. 1. In Situ Raman Spectroscopy and Ab Initio Molecular
13 Orbital Calculations, *J. Am. Chem. Soc.*, 120 (1998) 9041-9046, 25 B.
- 14 [31] Catalytic oxidation of phenol by hydrogen peroxide over a pillared clay containing
15 iron. Active species and pH effect, J. M. Tatibouët, E. Guérou et J. Fournier, *Topics*
16 *Catal.*, 33 (2005) 225-229
- 17 [32] J. Jia, W. Yang, P. Zhang, J. Zhang, Facile synthesis of Fe-modified manganese
18 oxide with high content of oxygen vacancies for efficient airborne ozone destruction,
19 *Appl. Catal. A: Gen.*, 546 (2017) 79-86
- 20 [33] G. Zhu, J. Zhu, W. Jiang, Z. Zhang, J. Wang, Y. Zhu, Q. Zhang, Surface oxygen
21 vacancy induced α -MnO₂ nanofiber for highly efficient ozone elimination, *Appl. Catal. B:*
22 *Env.*, 209 (2017) 729-737

1 [34] B. Dhandapani, S.T. Oyama, Gas phase ozone decomposition catalysts, Appl. Catal.
2 B Environ. 11 (1997) 129–166

3 [35] J.M. Tatibouët, Methanol oxidation as a catalytic surface probe, Appl. Catal. A: Gen.,
4 148 (1997) 213-252

5

6

7

8

9

10

11

12